AIMS Microbiology

AIMS Microbiology, 12(4): 774–788.
DOI: 10.3934/microbiol.2026033
Received: 04 May 2026
Revised: 15 October 2026
Accepted: 19 October 2026
Published: 29 October 2026

https://www.aimspress.com/journal/microbiology

Research article

The synergism of the antibacterial action of lysostaphin and warnerin, an antibacterial peptide of the epilancin group, against *Staphylococcus aureus*

Aleksandr Lobanov, Ekaterina Yaburova, Daria Eroshenko and Tatyana Polyudova*

Institute of Ecology and Genetics of Microorganisms, Perm, Russian Federation

* **Correspondence:** Email: polyudova@iegm.ru.

Abstract: Whole-genome sequencing of *Staphylococcus warneri* KL-1 (GenBank GCA_056393345.1) confirmed that this strain harbors a biosynthetic gene cluster encoding epilancins, a class I antimicrobial peptide known as a lantibiotic. The peptide warnerin produced by this strain belongs to the epilancin group and has a high degree of homology with epilancin A37, with a single substitution at position 8 (Val→Ile). Three studied *Staphylococcus aureus* strains, including MRSA, exhibited low sensitivity to warnerin (MICs 83.38–166.75 μM) and moderate sensitivity to lysostaphin (LS) (MICs 0.15–0.29 μM). However, the combination of LS and warnerin reduced the MIC of warnerin by 16-fold and that of LS by 16–32-fold, depending on the strain. Compared with untreated cells, exposure to subMIC warnerin did not affect cell viability but increased the release of K^+, ATP, and RNA, indicating disruption of membrane integrity. The synergistic interaction between warnerin and LS was confirmed by the fractional inhibitory concentration index and isobologram analyses and was associated with enhanced cell damage. The bactericidal effect of the combination was demonstrated using a time-kill assay. Morphological changes in *S. aureus* cells under the influence of warnerin, LS, and their combination were demonstrated via confocal microscopy and AFM.

Keywords: warnerin; synergism; pore formation; isobologram analysis; confocal microscopy; fractional inhibitory concentration

1. Introduction

The knowledge on the functional effects of staphylococci on skin has focused primarily on *Staphylococcus aureus*. The important role of coagulase-negative staphylococci (CoNS), the most

frequently isolated skin commensal, in skin health and homeostasis is increasingly becoming apparent. CoNS can exhibit direct antimicrobial activity through the production of antimicrobial peptides (AMPs), the serine protease Esp, acids, and quorum factors [1]. Among CoNS, AMP production is widespread, occurring in 1.4% to 6.4% of isolates, depending on the site of isolation [2,3].

The best-studied staphylococcal AMP is the 27 kDa lysostaphin (LS), which is secreted by *Staphylococcus simulans* and *Staphylococcus staphylolyticus*, and belongs to a class IIIa metalloprotease. The catalytic domain of LS has three distinct functions (a glycylglycine endopeptidase, an endo-β-N-acetylglucosaminidase, and an N-acetylmuramyl-L-alanine amidase), enabling it to cleave peptidoglycan components, particularly pentaglycine cross-bridges [4]. These structures are not typically seen in CoNS, making LS specific for actively growing and quiescent *S. aureus*. The minimum inhibitory concentrations (MICs) of LS for *S. aureus* isolates vary widely; however, the MICs of the most common susceptible strains range from 0.03–2.00 μg/mL [5,6], a value that has been consistent over the past 50 years [7,8].

Nevertheless, in a metabolically active state, particularly in nutrient-rich environments, some *S. aureus* strains exhibit high basal resistance mediated by teichoic acids, which are able to shield the cell surface by physically interfering with LS binding to its target. Moreover, repression or deletion of genes responsible for teichoic acid synthesis (*tarO*, *tarH*, and *tarG*) deprives the cell of protection and dramatically reduces the resistance of *S. aureus* to LS, even under growth-promoting conditions [9]. Furthermore, isolates may carry mutations in genes linked to the main target of LS. These include mutations affecting peptide cross-bridge truncation (*femA*, *femB*), serine modification (*fmhA*, *fmhC*), cell wall assembly regulation (*spdC*), or precursor pool disruption (*shmT*). Under physiological conditions, such isolates can display a significant increase in resistance, reaching complete insensitivity with MIC values exceeding 2.00 μg/mL [9–11].

Another important class of staphylococcal AMPs is class I lantibiotics, particularly epilancins. These peptides are characterized by the presence of lanthionine (Ala12-S-Ala16), a lactate-capped N-terminus, and ring systems B and C, which have high affinity for the D and E rings of nisin [12]. Unlike nisin, however, epilancins do not bind lipid II in the cell wall. According to bioinformatics data, epilancin genes are frequently harbored by different CoNS species (*S. epidermidis*, *S. hominis*, *S. warneri*, *S. casei*, and *S. xylosus*), which demonstrates the adaptive capacity of CoNS strains and pronounced interspecific competition and suggests the high ecological significance of lantibiotics [13]. Studies show that the presence of CoNS antagonists in the skin microbiome leads to the inhibition of *S. aureus* skin colonization [1,14]. Notably, epilancin E from *S. epidermidis* C33 was shown to be active against MRSA using spot-on-lawn assays [15]. However, the resistance of several *S. aureus* strains to epilancin A37 and K7 has been demonstrated *in vitro* [13,16]. The difference in susceptibility of *S. aureus* strains to epilancins may be related to differences in the expression levels of the multiple peptide resistance factor (MprF) and teichoic acid alanylation genes, which are associated with the *dlt* operon and with a reduction in the overall negative charge of cells [17]. Notably, mutants of the *dlt* operon genes lacking alanine in teichoic acids are more sensitive to LS [18].

The synergistic effects of LS and several AMPs, such as nisin, colistin, polymyxin B, and magainin, on MSSA and MRSA have been described [19]. Synergism between LS and the human cathelicidin LL-37 has also been established against *S. aureus* [20]. However, the synergism between lysostaphin and staphylococcal AMPs, as well as their mechanisms of action, remain poorly understood.

Previously, we isolated the peptide warnerin from the culture medium of *S. warneri* KL-1 [21]. This lantibiotic exhibits potent antibacterial activity against the highly susceptible indicator strain *S. cohnii*

VKM-3165, which lacks the *mprF* gene and possesses a nonfunctional *dlt* operon [22]. The mechanism of action of warnerin against CoNS is associated with disruption of the membrane potential, leakage of K^+ ions and ATP, generation of reactive oxygen species, and activation of bacterial autolysins [23].

Therefore, to understand the role of AMPs in maintaining the microbiota on human skin, we performed a complete genome analysis of the warnerin-producing strain *S. warneri* KL-1 and identified a cluster of AMP genes similar to epilancin genes, followed by an assessment of the combined effect of warnerin and LS against *S. aureus*.

2. Materials and methods

2.1. Microorganisms and culture conditions

Three *S. aureus* reference strains (ATCC 25923, ATCC 9144, and ATCC 43300) were used. Cultures were grown overnight at 37 ℃ in lysogeny broth (LB; Hopebio, China).

2.2. Antimicrobial peptides

Lysostaphin (LS) from *Staphylococcus staphylolyticus* (MW 26,926 Da) was obtained from Sigma-Aldrich (USA). A 0.5 mg/mL (18.6 μM) stock solution was prepared in either sterile Milli-Q water or Mueller-Hinton broth (MHB). Warnerin (MW 2998.6 Da; APD ID: AP02801) was isolated from the growth medium of *S. warneri* KL-1 (DSMZ 16081) and purified as described in [21]. The peptide was reconstituted in Milli-Q water or MHB (2 mg/mL; 667 μM) and sterile-filtered via a 0.22 μm syringe filter (33 mm diameter) to ensure solution stability. All stock solutions were stored at 4 ℃, and working dilutions were prepared immediately before use.

2.3. Sequencing and DNA analysis

Whole-genome sequencing of the *S. warneri* KL-1 strain was performed on the GeneMind FASTA Seq 300 platform in paired-end mode (2 × 150 bp). Read quality assessment was carried out via FastQC (version 0.12.1), and read trimming was performed via the cutadapt tool (version 5.0).

De novo genome assembly was conducted via the SPAdes algorithm (version 4.2) [24]. Assembly quality was assessed via Quast (version 5.3.0) [25] and CheckM (version 1.2) [26]. The final sequencing depth was 122×. Genome annotation was performed via two pipelines: Prokka (version 1.14) [27] and Bakta (version 1.11) [28].

For detailed gene-by-gene searches, the Basic Local Alignment Search Tool (BLAST) algorithm available through the National Center for Biotechnology Information (NCBI) portal was used. The identification of biosynthetic gene clusters (BGCs) was carried out via the online platforms antiSMASH version 8.0 [29] and BAGEL4 [30]. Analysis of the obtained genome assembly was performed with the default settings recommended for the detection of lantibiotics and other RiPPs (ribosomally synthesized and posttranslationally modified peptides). Cluster boundary localization, gene organization, and homology to known sequences were assessed via tools integrated into the aforementioned platforms, as well as via comparisons with the MIBiG database version 4 [31].

2.4. Broth Microdilution Assay

Minimal inhibitory concentrations (MICs) were determined by the broth microdilution method according to CLSI guidelines [32]. Twofold serial dilutions of LS and warnerin were prepared in 96-well polystyrene microplates, with maximum concentrations of 18.57 μM and 667 μM, respectively. The inoculated plates were incubated at 37 ℃ for 24 h. The MIC was defined as the lowest antimicrobial concentration that inhibited visible bacterial growth.

2.5. Checkerboard Assays

The combined activity of LS and warnerin was evaluated using the checkerboard MIC method as described in [33]. Twofold serial dilutions of LS and warnerin were prepared in MHB, with maximum concentrations of 2.32 μM and 333.5 μM, respectively. Drug combinations were obtained by mixing LS and warnerin at a 1:1 ratio. Each well was inoculated with 10 μL of bacterial suspension (10^6 CFU/mL) and incubated at 37 ℃ for 18–20 h. Wells without antibacterial agents served as growth controls. Bacterial viability was assessed by adding 10 μL of 0.1% thiazolyl blue tetrazolium bromide (Sigma, USA), followed by a 1 h incubation.

The fractional inhibitory concentration index (FICI) was calculated as $FICI = FIC_A + FIC_B$, where FIC_A = MIC of drug A in combination/MIC of drug A alone and FIC_B = MIC of drug B in combination/MIC of drug B alone. The FICI values were interpreted as synergistic (≤0.5), additive (>0.5–1.0), indifferent (>1.0–4.0), or antagonistic (>4.0).

2.6. Time-kill kinetic analysis

Bacterial suspensions (10^6 CFU/mL) were prepared in 10 mM Tris-HCl buffer (pH 7.2). LS was added at 0.25 × MIC, and warnerin was added at 1 × FIC. The samples were incubated at 37 ℃, and aliquots were collected at 0, 1, 3, and 24 h. Viable counts (CFU/mL) were determined by serial decimal dilution followed by plating on agar media.

2.7. Microscopic examination of Staphylococcus cells

The bacterial cell morphology of *S. aureus* ATCC 25923 exposed to LS (0.25 × MIC—0.07 μM) or warnerin (1 × FIC—5.21 μM) alone or in combination was analyzed via an Olympus FV 1000 confocal laser scanning microscope (CLSM) (Olympus Corporation, Tokyo, Japan) and an Asylum MFP-3D atomic force microscope (AFM) (Asylum Research, Santa Barbara, CA, USA).

The membrane integrity of *S. aureus* ATCC 25923 after 3 h of treatment was assessed via CLSM. The glass slide containing the sample was air-dried for 10–15 min, after which the fluorescent dye LIVE/DEAD BacLight Bacterial Viability Kit (Thermo Fisher Scientific, USA) was added, and the sample was left in the dark for 15–20 min. The preparation was washed with deionized water to remove residual dye. CLSM scanning was performed using an immersion objective (100×, numerical aperture 1.4), an argon laser (λ = 488 nm) with a 505/525 nm barrier filter and a helium-neon laser (λ = 543 nm) with a 560/660 nm barrier filter.

AFM scanning was performed in semicontact mode in air using an AC240TS silicon cantilever with a resonance frequency of 50–90 kHz and a contact stiffness of 2 N/m. Images were analyzed via

the FV10-ASW 3.1 program (Olympus Corporation, Tokyo, Japan) and AFM software (Igor Pro 6/22A Wave Metrics, Portland, OR, USA).

2.8. Evaluation of the effects of lysostaphin and warnerin on membrane integrity

Following treatment with LS, warnerin, or their combination, *S. aureus* ATCC 25923 cells suspended in 10 mM Tris-HCl buffer were harvested by centrifugation (12,000 × g, 10 min). The resulting supernatants were collected to quantify the leakage of intracellular components. The concentrations of genomic DNA and total RNA were determined via a Qubit™ fluorometer with DNA BR and RNA Assay Kits (Invitrogen, USA), respectively. Extracellular ATP levels were measured via the RealTime-Glo™ Extracellular ATP Assay (Promega, USA) on a Luminoskan TL Plus luminometer (Thermo, USA). The concentration of potassium ions (K^+) was quantified via a Shimadzu AA-7000 atomic absorption spectrometer (Shimadzu, Japan). All the measurements were performed in accordance with the manufacturers' instructions. A buffer containing the respective peptides without bacterial cells served as a negative control to account for background interference.

2.9. Statistical analysis

All experiments were performed with at least three biological replicates. Data visualization and curve fitting were performed via Prism 10.4 software for Windows (GraphPad Software, Inc.). The means were analyzed by one-way analysis of variance (ANOVA) followed by Tukey's post hoc multiple comparison test. The results are expressed as the mean ± standard deviation (SD), and a P value < 0.05 was considered to indicate statistical significance.

3. Results and discussions

3.1. Whole-genome sequencing analysis

Whole-genome sequencing confirmed that strain KL-1 was an *S. warneri* strain (GenBank GCA_056393345.1), and the genome size was 2,497,625 bp (24 contigs), with a GC content of 32.52%. Genome annotation identified 2,489 genes, including 59 tRNA and 4 rRNA sequences (three 5S rRNA, four 16S rRNA, and four 23S rRNA). The biosynthetic gene cluster (BGC) of *S. warneri* KL-1 is highly similar to those described for epilancin A37 [13], K7 [34], and 15X [35]. The organization of the BGC of *S. warneri* KL-1 is similar to the structure described for *S. epidermidis* 15X154 [35]. Therefore, the warnerin BGC also consists of typical genes: a precursor peptide (*elkA*), a protease (*elkP*), a transporter protein (*elkT*), three tailoring enzymes (*elkBCO*), and three putative immunity proteins (*elkI1*, *elkI2*, and *elkI3*).

Based on the conserved nature of posttranslational modification among epilancins [35], we predicted the structure of warnerin, which is presented alongside epilancins A37 [13], K7 [34], and 15X [35] in Figure 1. Notably, all these epilancins share a common N-terminal fragment capped by a lactate residue, followed by highly conserved modified amino acid residues dehydroalanine (Dha) and dehydrobutyrine (Dhb). A five-membered lanthionine ring connected via a short three-residue hinge to a second ring system, consisting of two intertwined four-membered lanthionine rings and a short six-residue C-terminus, is characteristic of all the peptides compared. The structure of warnerin shares

these conserved structural motifs (an N-terminal lactate residue, three lanthionine-type rings, and the dehydrated residues Dha and Dhb) but differs from epilancin A37 by a single amino acid substitution and from K7 and 15X at multiple positions (Figure 1).

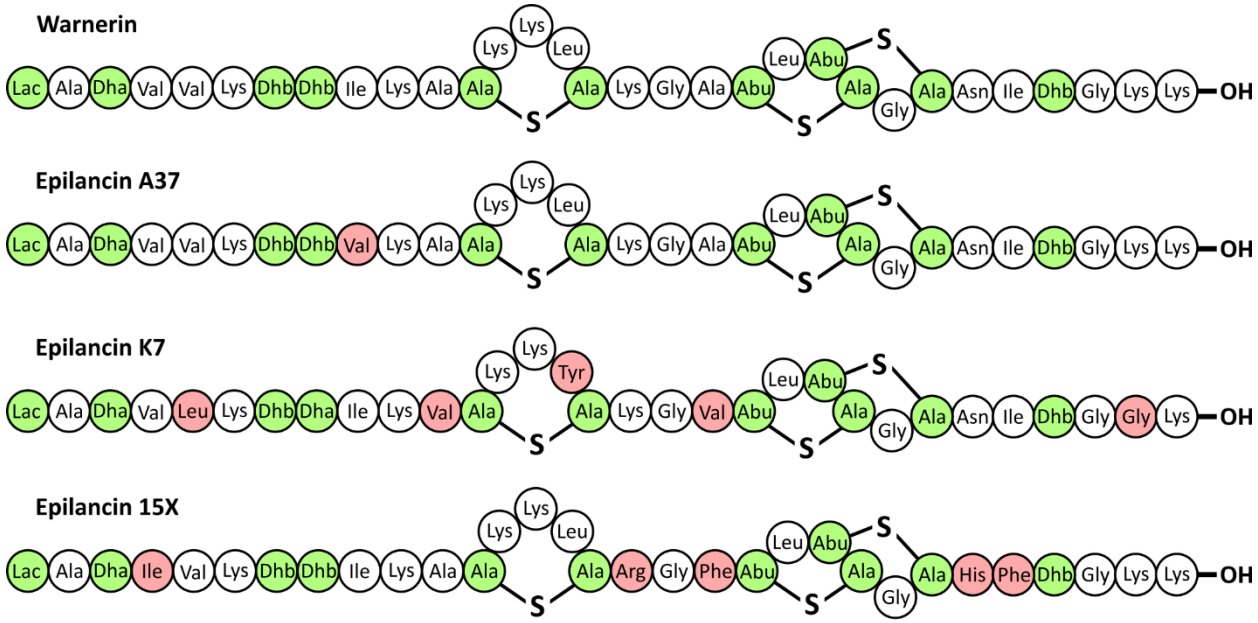


Figure 1. Predicted structures of warnerin, A37 [13], K7 [34], and 15X [35]. Green: posttranslationally modified residues: Dha—dehydroalanine, Dhb—dehydrobutyrine, Abu—α-aminobutyric acid. Red: residue substitution.

The calculated molecular mass of warnerin was 2998.6 Da, which is consistent with the mass spectrometry data [21]. Thus, warnerin is a lantibiotic of the epilancin group, and its structure is most similar to that of epilancin A37.

3.2. Minimum inhibitory concentrations (MICs) of warnerin and LS against S. aureus

There is no defined or officially accepted MIC value for LS that could be used as a susceptibility breakpoint. Some authors, such as Kusuma et al. [36], classify staphylococci as resistant to LS when the MIC value exceeds 1.19 μM (32 μg/mL); however, the most common susceptible strains have MICs in the range of 0.03–2.00 μg/mL [5,6]. All tested *S. aureus* strains, including the MRSA strain *S. aureus* ATCC 43300, showed moderate susceptibility to LS and low susceptibility to warnerin (Table 1). Specifically, the MIC values of LS ranged from 0.15 to 0.29 μM (3.9 to 7.8 μg/mL), whereas warnerin inhibited *S. aureus* growth only at substantially higher concentrations of 83–166 μM (250–500 μg/mL).

Table 1. Minimum inhibitory concentrations of lysostaphin and warnerin for *S. aureus* (μM).

	S. aureus ATCC 25923	*S. aureus* ATCC 9144	*S. aureus* ATCC 43300
Lysostaphin	0.29	0.29	0.15
Warnerin	83.38	83.38	166.75

To explain the differences in the MICs of LS and warnerin for the *S. aureus* strains studied, we analyzed the presence and mutations of the genes associated with the synthesis of peptidoglycan and teichoic acids *(femA*, *femB*, *femX* (*fmhB*), *fmhA*, *fmhC*, *lyrA*, *glyA*, *tarO*, *tarH*, *tarG*, *mprF*, and *dltABCD*) via the BLASTn algorithm (Tables S1 and S2). The genomes of *S. aureus* ATCC 25923, ATCC 9144, and ATCC 43300 (GCA_000756205.1, GCA_047376985.1, and GCF_047391735.1, respectively) harbor intact copies of the *femA*, *femB*, and *femX* (*fmhB*) genes, which are responsible for the synthesis of the pentaglycine cross-bridge [37], suggesting high sensitivity to LS. The *fmhA* gene, encoding an enzyme that incorporates Gly-Ser dipeptides into cross-bridges, is intact in the genomes of *S. aureus* ATCC 9144 and *S. aureus* ATCC 43300 but is represented by a pseudogene in the *S. aureus* ATCC 25923 genome. Inactivation of *fmhA* can cause minor changes in staphylococcal peptidoglycan, resulting in increased susceptibility to LS [10]. However, despite the presence of defects in the gene potentially contributing to LS resistance in *S. aureus* ATCC 25923, this strain had an MIC of LS equal to the MIC of *S. aureus* ATCC 9144 harboring the full *fmhA* gene (Table 1). Therefore, resistance to LS likely requires specific inducing stimuli [36]. The lowest MIC of LS for *S. aureus* ATCC 43300 (0.15 μM) may be related to the presence of a defective *tarO* gene in this strain. Disruption of *tarO* may affect cell wall integrity and increase susceptibility to antimicrobial agents, including LS [9]. The resistance of *S. aureus* to epilancins may be associated with the action of the multiple peptide resistance factor (MprF) and the shielding of the negative charges of teichoic acids by alanine, which is mediated by the *dlt* operon [17]. The presence of these intact modification systems in the genomes of all the studied strains correlates with high MIC values of warnerin (>80 μM) (Table 1) and suggests the functional activity of these defense mechanisms.

3.3. Checkerboard assay for LS and warnerin

Studies have shown that combinations of LS with cationic antimicrobial peptides have a synergistic effect on *S. aureus* [19,20] because LS increases the susceptibility of *S. aureus* to a wide range of antimicrobial compounds.

A checkerboard assay was performed to confirm the synergistic activity of LS and warnerin. In this study, warnerin alone was not able to achieve desirable bacterial inhibition, as indicated by a high MIC value (83–166 μM) (Table 1). However, in the presence of subMICs of LS, the antibacterial effect of warnerin increased, leading to a significant reduction in its MIC against *S. aureus* (Figure 2A–C). The FICs of warnerin and LS in combination were 5.21 μM and 0.009–0.018 μM, respectively, against *S. aureus* ATCC 9144 and *S. aureus* ATCC 25923, whereas they were 10.42 μM and 0.005 μM, respectively, against *S. aureus* ATCC 43300 (Table 2).

Thus, the MIC of warnerin in combination was reduced by 16 times for all the tested *S. aureus* strains. Similarly, the FICs of LS in combination were reduced by 16–32 times for the target strains. The calculated fractional inhibitory concentration index (FICI) for the LS and warnerin combinations for all *S. aureus* strains tested was 0.09–0.13, which indicates that the synergistic effect between LS and warnerin strongly inhibits bacterial growth (Table 2). In addition to presenting the FICI values, isobologram plots were created to visually evaluate the interactions between LS and warnerin (Figure 2D–F). Isobolographic analysis is one of the methods used to assess the pharmacodynamic interactions between drugs. By plotting fractional inhibitory concentrations on a Cartesian coordinate system, this method distinguishes synergistic, additive, and antagonistic interactions: Data points falling below the line of additivity indicate synergism, whereas those above the line indicate antagonism [38]. Isobologram analysis

confirmed a strong synergistic interaction between LS and warnerin across all tested *S. aureus* strains, as all experimental FIC points fell well below the line of additivity and the theoretical synergy threshold.

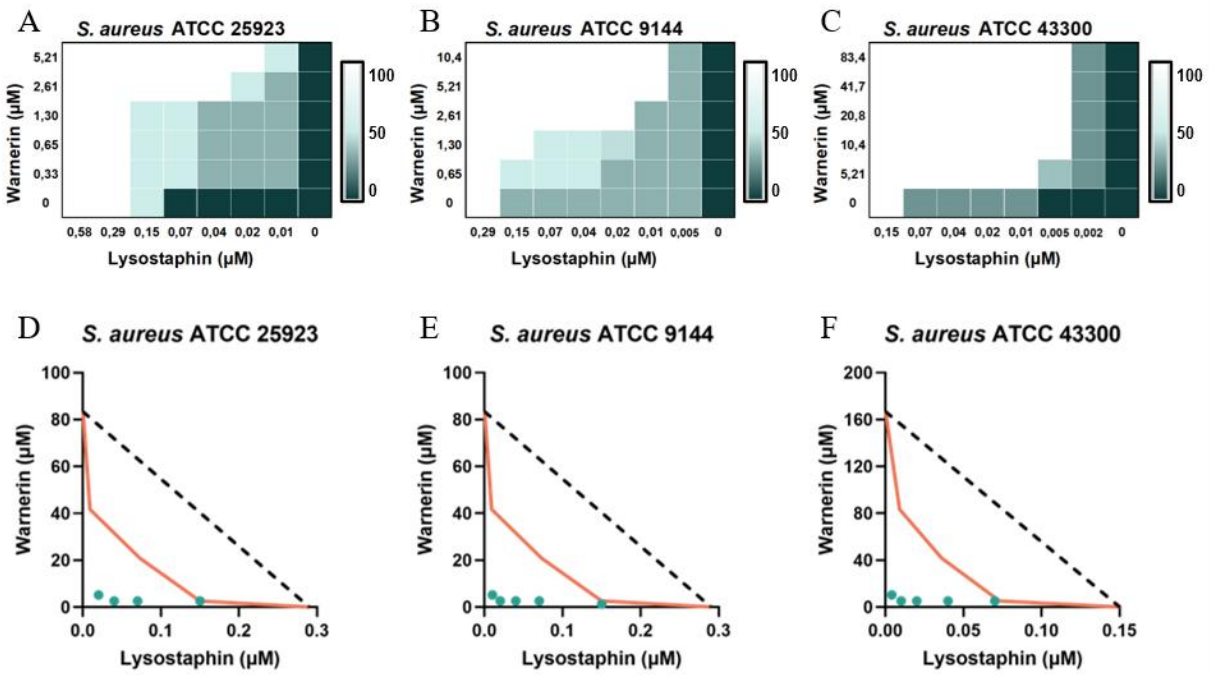


Figure 2. Evaluation of the combined efficacy of LS and warnerin against *S. aureus* ATCC 25923 (A,D), *S. aureus* ATCC 9144 (B,E), and *S. aureus* ATCC 43300 (C,F): Checkerboard analysis and isobolograms. (A–C) Heatmaps of the checkerboard microdilution assays. Lighter colors indicate greater bacterial inhibition. (D–F) Isobologram analysis of the interaction between warnerin and LS. The dashed line represents the line of additivity. The orange curve indicates the theoretical synergism threshold, whereas the green circles denote the observed experimental values obtained via the checkerboard method. Checkerboard assays were performed using three independent biological replicates (n = 3). The heatmaps and isobolograms show the mean results obtained for the tested concentration combinations.

Table 2. Fractional inhibitory concentration index (FICI) values for LS and warnerin combinations against *S. aureus*.

	S. aureus ATCC 25923	*S. aureus* ATCC 9144	*S. aureus* ATCC 43300
FIC of LS/Warnerin, µM	0.018/5.21	0.009/5.21	0.005/10.42
FICI	0.13 (S)	0.09 (S)	0.09 (S)

(S): Synergy ≤ 0.5; (Ad): Additive > 0.5–1; (I): Indifferent 1.0– ≤ 4.0

3.4. Time-kill kinetic analysis

A time-kill assay of all tested *S. aureus* strains with the LS and warnerin combination was conducted

to further confirm their synergistic and bactericidal effects. The 0.25 × MIC of LS alone did not cause a significant decrease in the number of living cells (Figure 3). In contrast, warnerin alone at 1 × FIC initially reduced viable cell counts by 1–2 log CFU/mL compared with the initial inoculum, although bacterial regrowth was observed for *S. aureus* ATCC 9144 and ATCC 43300 after 24 h (Figure 3B,C), possibly due to proteolytic degradation of warnerin [33]. However, the combined action of LS (0.25 × MIC) and warnerin (1 × FIC) caused a > 4 log CFU/mL reduction in viable cell counts over 24 h, indicating that the combination is bactericidal rather than bacteriostatic.

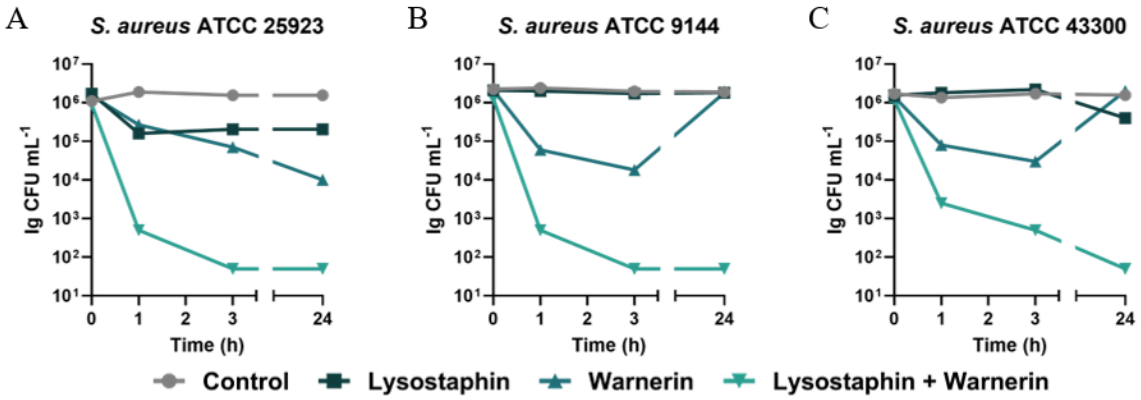


Figure 3. Time-kill curves of *S. aureus* ATCC 25923 (A), *S. aureus* ATCC 9144 (B), and *S. aureus* ATCC 43300 (C) at LS (0.25 × MIC) and warnerin (1 × FIC) alone or in combination. A representative example of three biological replicates is shown.

3.5. Cell permeability of S. aureus ATCC 25923

The synergistic bactericidal activity of the combination of LS and warnerin could result from the ability of LS to degrade the cell wall and increase the accessibility of the peptide to the cell membrane [19]. Nevertheless, the actual mechanism of the synergy between lysostaphin and warnerin is not fully known. For this study, a suspension of *S. aureus* ATCC 25923 with a relatively high cell count (10^8 CFU/mL) was used, while the concentrations of warnerin and LS remained the same as those used in the previous experiments; 1 × FIC and 0.25 × MIC, respectively. CLSM of *S. aureus* ATCC 25923 after 3 h of treatment alone or in combination with live/dead staining (Figure 4A–D) revealed disruption of the membrane permeability of staphylococcal cells under the influence of subMICs of LS (Figure 4B). The AFM images also revealed that *S. aureus* ATCC 25923 lost its spherical shape and turgor and shrunk upon LS treatment (Figure 4F), which corresponds to the data shown earlier [11]. The LS treatment promoted osmotic instability in the cells, which resulted in the release of K^+ ions, ATP, RNA (Figure 4J–L), and DNA (Figure S1) into the extracellular medium.

After treatment with warnerin, no obvious cell damage was observed, but the intensity of green staining was significantly lower than that in untreated cells (Figure 4C). However, the AFM images of staphylococcal cells treated with warnerin alone revealed that these cells were phenotypically comparable to untreated controls (Figure 4E,G). Apparently, warnerin at the tested concentration (1 × FIC) did not induce the formation of pores sufficient for the penetration of the PI dye, as was also shown for epilancin A37 [13]. Furthermore, intense potassium and ATP leakage were observed after just 30 min of exposure

to warnerin alone (Figure 4J,K), as was RNA release (Figure 4L), but not DNA release (Figure S1). This indicates that the formation of small pores and the membrane-damaging activity of warnerin alone are insufficient to cause cell death and may lead to cell regrowth after 24 h (Figure 3B,C). In the case of *S. cohnii* VKM-3165, warnerin, in addition to membrane-damaging activity, has the ability to activate autolysins, which cause abrupt cell lysis [23]. However, *S. aureus* possesses the *mprF* and *dlt* systems, which are responsible for the aminoacylation of membrane phospholipids and alanylation of teichoic acids, respectively, [17] in contrast to *S. cohnii* VKM-3165, which lacks the *mprF* gene and has a non-functional *dlt* operon [22]. These modifications reduce the negative charge of the bacterial cell surface and, consequently, the electrostatic attraction of cationic peptides and enable stabilizing cell wall proteins, including autolysins, as demonstrated for adhesins [39]. Moreover, the presence of aminoacylated phospholipids likely increases membrane rigidity [40] and prevents their vesiculation, which is an important part of the mechanism of action of both warnerin [23] and the almost identical epilancin A37 [13] in *mprF*-negative bacteria. According to data from the NCBI database, the three studied collection strains of *S. aureus* (ATCC 25923, ATCC 9144, and ATCC 43300) contain a functional *mprF* gene and *dlt* operon (assembly numbers: GCA_000756205.1, GCA_047376985.1, and GCA_047391735.1) (Table S2). Therefore, a larger collection of clinical *S. aureus* isolates with diverse phenotypes is needed for future validation. Notably, increasing the dose of warnerin to 1 × MIC led to a significant increase in the membrane permeability of *S. aureus* ATCC 25923 for PI, but the number of viable cells was still similar to that of untreated cells after 1 h (Figure S2).

Treatment with the combination of LS and warnerin markedly increased the proportion of membrane-compromised (PI-positive, red) cells while substantially reducing the total number of intact cells in the field of view (Figure 4D). Compared with either agent alone, the combination induced pronounced damage to the cell wall and cytoplasmic membrane of *S. aureus* ATCC 25923, leading to elevated leakage of K^+ ATP, RNA (Figure 4J–L), and DNA (Figure S1). AFM imaging confirmed extensive cell lysis, evidenced by sparse remaining cells surrounded by abundant cellular debris following combined treatment (Figure 4H). Furthermore, the surviving cells no longer formed typical grape-like clusters, appearing instead as single cells, pairs, or tetrads. Propidium iodide-permeable cells exhibited no apparent morphological damage in AFM images; however, compared to untreated cells, they showed a ~25% reduction in mean size (318.8 nm vs. 423.7 nm; n = 30) and a ~35% decrease in maximum height (467.0 nm vs. 722.3 nm; n = 30). We have shown that warnerin stimulates the activation of autolysins in susceptible *S. cohnii* VKM-3165, dramatically increasing the bactericidal activity of warnerin [23]. However, at a higher cell density (~10^8 CFU/mL), single subMIC treatments of warnerin or LS showed negligible bactericidal activity against *S. aureus*. Under these conditions, a visible reduction in cell viability (>2 log CFU/mL) was achieved only when warnerin was combined with LS, which acts as an exogenous peptidoglycan hydrolase (Figure 4I).

Therefore, the proposed mechanism of the combined action likely involves warnerin-induced pore formation in the *S. aureus* cytoplasmic membrane without significant activation of endogenous autolysins when applied alone, as the peptidoglycan layer remains intact. Concurrently, additional experiments demonstrated that LS promoted endogenous autolysis in viable *S. aureus* ATCC 25923 cells while causing only minor lysis in heat-killed bacteria, in which endogenous peptidoglycan hydrolases had been thermally inactivated (Figure S3). Thus, the combined action of subMIC LS and warnerin not only compromises membrane integrity but also accelerates cell wall degradation, potentially mediated by autolysin activation, thereby enhancing bactericidal activity and the leakage of intracellular components.

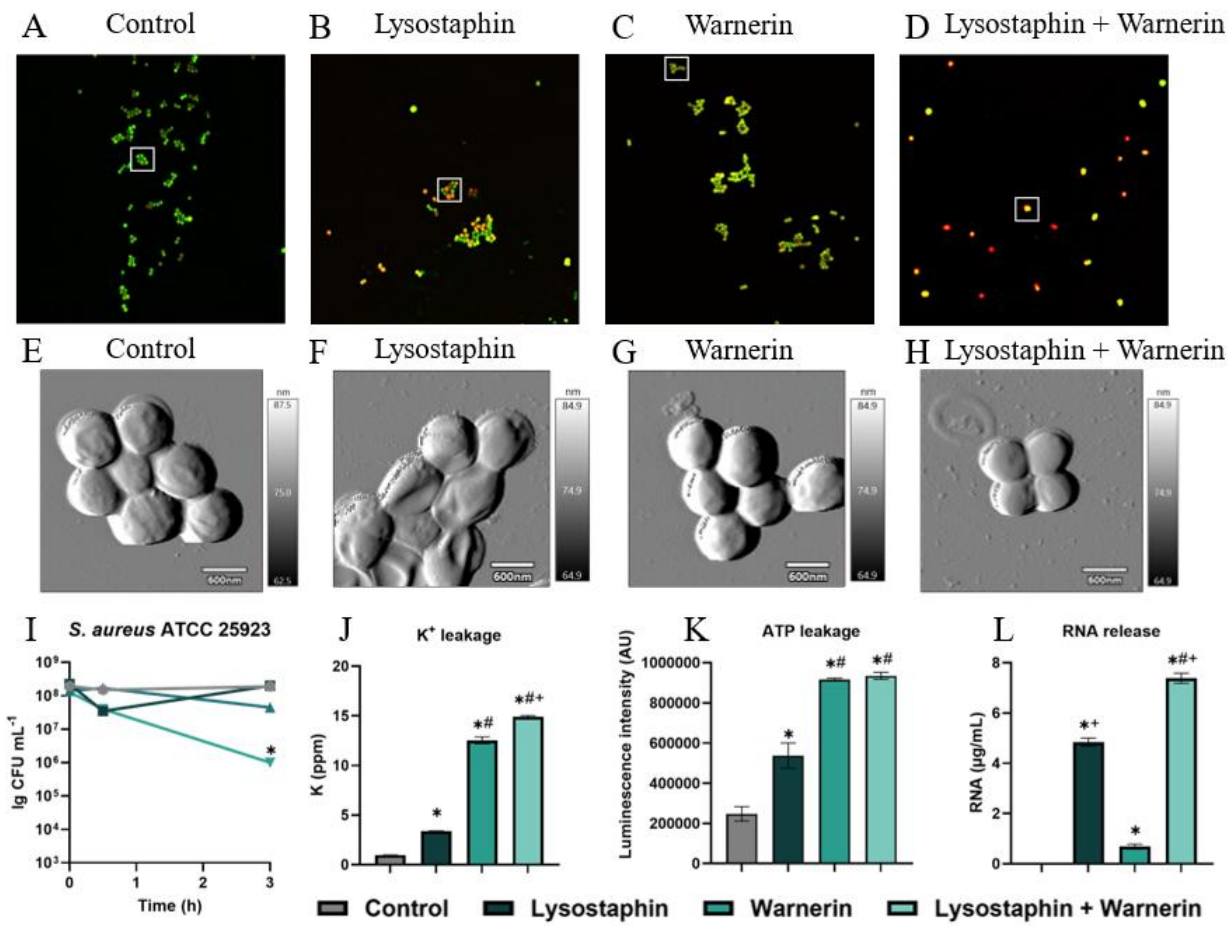


Figure 4. The synergistic bactericidal activity of the combination of LS and warnerin against *S. aureus* ATCC 25923. (A–D) CLSM images of *S. aureus* ATCC 25923 after live/dead staining: untreated (A) and after treatment for 3 h with LS (B), warnerin (C), or their combination (D). Green staining (SYTO9) corresponds to cells with an intact membrane. Red staining (propidium iodide) corresponds to cells with a damaged membrane. The white squares indicate the areas selected for AFM analysis. (E–H) AFM images of *S. aureus* ATCC 25923: Untreated (E) and after treatment for 3 h with LS (F), warnerin (G), or their combination (H). (I–L) Quantitative data presented from 3 independent biological replicates. (I) Time-kill curves over 3 h for the control (gray), 0.25 × MIC of LS (dark green), 1 × FIC of warnerin (teal), and the combination (light green). (J–L) Leakage of potassium (J), ATP (K), and RNA (L) from *S. aureus* ATCC 25923 cells: Intact cells (gray); after 30 min of treatment with LS (dark green), warnerin (teal), or their combination (light green). All quantitative data are expressed as means ± SDs from 3 independent experiments. Statistical significance was evaluated using ANOVA test. * $p < 0.05$ vs. control; # $p < 0.05$ vs. lysostaphin; + $p < 0.05$ vs. warnerin (for interpretation of the references to color in this figure legend, the reader is referred to the web version of this article).

Several limitations of this study should be noted. First, the experiments were conducted using only three reference *S. aureus* strains (two MSSA and one MRSA). Given the genetic and phenotypic diversity of clinical *S. aureus* strains, particularly regarding cell envelope charge modifications (*mprF*

and *dltABCD*) and peptidoglycan cross-bridge structure, further validation using a broader panel of clinical isolates is required. Second, the precise contribution of endogenous *S. aureus* autolysins to the synergistic bactericidal effect remains to be fully elucidated. Finally, as all assays were performed *in vitro*, future *ex vivo* and *in vivo* studies, including cytotoxicity and immunogenicity evaluations, are necessary to assess whether this combination holds potential for topical or clinical applications.

4. Conclusions

This study demonstrates, for the first time, the *in vitro* synergistic interaction between LS, a potent antistaphylococcal enzyme, and warnerin, an epilancin-group lantibiotic, against reference strains of *S. aureus*. Combining LS with warnerin markedly enhanced antibacterial efficacy, reducing the effective concentration of LS by 16–32-fold and that of warnerin by 16-fold. Although such dose reductions could theoretically help mitigate concentration-dependent limitations of LS, further validation across a wider range of clinical isolates and *in vivo* models is required to evaluate the practical applicability of this combination. Mechanistically, the observed synergy arises from a dual-target mode of action affecting the cytoplasmic membrane (targeted by warnerin) and the peptidoglycan network (targeted by LS), resulting in a pronounced bactericidal effect. Specifically, subMIC warnerin induces the formation of small membrane pores, leading to K^+ and ATP leakage, dissipation of the membrane potential, and disruption of energy metabolism without causing immediate cell death. Moreover, LS compromises the peptidoglycan layer, leading to a loss of spherical shape and turgor pressure, accompanied by the release of K^+, ATP, and RNA. Consequently, warnerin-induced membrane depolarization and ATP depletion likely impair the ability of *S. aureus* to repair LS-mediated cell wall damage, while the combination may also facilitate autolysin activation normally restrained by alanylated teichoic acids. Overall, these findings expand our understanding of the mechanism of action of epilancins produced by CoNS and suggest their potential ecological role in interspecies competition and the modulation of *S. aureus* colonization within the human skin microbiota.

Use of AI tools declaration

The authors declare they have not used Artificial Intelligence (AI) tools in the creation of this article.

Conflict of interest

The authors declare no conflict of interest.

Author contributions

Aleksandr Lobanov: Writing—original draft, Writing—review & editing, Investigation, Formal analysis, Data curation, Visualization. Ekaterina Yaburova: Writing—review & editing, Formal analysis. Daria Eroshenko: Writing—review & editing, Conceptualization. Tatyana Polyudova: Writing—original draft, Writing—review & editing, Supervision, Resources, Methodology, Investigation.

Acknowledgments

This research was carried out on the basis of the Center for Collective Use "Research of Materials and Substances" of the Perm Federal Research Center, Ural Branch of the Russian Academy of Sciences. The authors acknowledge the Interdisciplinary Center for Shared Facilities of Kazan Federal University for performing whole-genome sequencing.

This work was supported by the Ministry of Science and Higher Education of the Russian Federation (124020500028-4).

References

1. Bier K, Schittek B (2021) Beneficial effects of coagulase-negative Staphylococci on *Staphylococcus aureus* skin colonization. *Exp Dermatol* 30: 1442–1452. https://doi.org/10.1111/exd.14381
2. Fernández-Fernández R, Lozano C, Eguizábal P, et al. (2022) Bacteriocin-like inhibitory substances in staphylococci of different origins and species with activity against relevant pathogens. *Front Microbiol* 13. https://doi.org/10.3389/fmicb.2022.870510
3. Polyudova TV, Lemkina LM, Antip'eva MV, et al. (2024) Prevalence of production of antagonism peptide factors among coagulase-negative staphylococci. *Microbiology* 93: 847–854. https://doi.org/10.1134/S0026261724606626
4. Gründling A, Missiakas DM, Schneewind O (2006) *Staphylococcus aureus* mutants with increased lysostaphin resistance. *J Bacteriol* 188: 6286–6297. https://doi.org/10.1128/JB.00457-06
5. Yang XY, Li CR, Lou RH, et al. (2007) *In vitro* activity of recombinant lysostaphin against *Staphylococcus aureus* isolates from hospitals in Beijing, China. *J Med Microbiol* 56: 71–76. https://doi.org/10.1099/jmm.0.46788-0
6. Szweda P, Schielmann M, Frankowska A, et al. (2014) Antibiotic resistance in *Staphylococcus aureus* strains isolated from cows with mastitis in eastern Poland and analysis of susceptibility of resistant strains to alternative nonantibiotic agents: Lysostaphin, nisin and polymyxin B. *J Vet Med Sci* 76: 355–362. https://doi.org/10.1292/jvms.13-0177
7. Harrison EF, Cropp CB (1965) Comparative *in vitro* activities of lysostaphin and other antistaphylococcal antibiotics on clinical isolates of *Staphylococcus aureus*. *Appl Microbiol* 13: 212–215. https://doi.org/10.1128/am.13.2.212-215.1965
8. Gordina EM, Bozhkova SA, Labutin DV, et al. (2023) Anti-staphylococcal activity and cytocompatibility of lysostaphin. *Clin Microbiol Antimicrob Chemother* 25: 77–82. https://doi.org/10.36488/cmac.2023.1.77-82
9. Wu X, Zha J, Koffas MAG, et al. (2019) Reducing *Staphylococcus aureus* resistance to lysostaphin using CRISPR-dCas9. *Biotechnol Bioeng* 116: 3149–3159. https://doi.org/10.1002/bit.27143
10. Willing S, Dyer E, Schneewind O, et al. (2020) FmhA and FmhC of *Staphylococcus aureus* incorporate serine residues into peptidoglycan cross-bridges. *J Biol Chem* 295: 13664–13676. https://doi.org/10.1074/jbc.RA120.014371
11. Batool N, Ko KS, Chaurasia AK, et al. (2020) Functional identification of serine hydroxymethyltransferase as a key gene involved in lysostaphin resistance and virulence potential of *Staphylococcus aureus* strains. *Int J Mol Sci* 21: 9135. https://doi.org/10.3390/ijms21239135

12. Wang X, Gu Q, Breukink E (2020) Non-lipid II targeting lantibiotics. *Biochim Biophys Acta Biomembr* 1862: 183244. https://doi.org/10.1016/j.bbamem.2020.183244
13. Puls JS, Winnerling B, Power JJ, et al. (2024) *Staphylococcus epidermidis* bacteriocin A37 kills natural competitors with a unique mechanism of action. *ISME J* 18: wrae044. https://doi.org/10.1093/ismejo/wrae044
14. Nakatsuji T, Chen TH, Narala S, et al. (2017) Antimicrobials from human skin commensal bacteria protect against *Staphylococcus aureus* and are deficient in atopic dermatitis. *Sci Transl Med* 9: eaah4680. https://doi.org/10.1126/scitranslmed.aah4680
15. Twomey E, O'Connor PM, Coffey A, et al. (2024) Inhibition of clinical MRSA isolates by coagulase negative staphylococci of human origin. *Antibiotics* 13: 338. https://doi.org/10.3390/antibiotics13040338
16. Varella Coelho ML, Santos Nascimento JD, Fagundes PC, et al. (2007) Activity of staphylococcal bacteriocins against *Staphylococcus aureus* and *Streptococcus agalactiae* involved in bovine mastitis. *Res Microbiol* 158: 625–630. https://doi.org/10.1016/j.resmic.2007.07.002
17. Joo HS, Otto M (2015) Mechanisms of resistance to antimicrobial peptides in staphylococci. *Biochim Biophys Acta Biomembr* 1848: 3055–3061. https://doi.org/10.1016/j.bbamem.2015.02.009
18. Peschel A, Vuong C, Otto M, et al. (2000) The D-alanine residues of *Staphylococcus aureus* teichoic acids alter the susceptibility to vancomycin and the activity of autolytic enzymes. *Antimicrob Agents Chemother* 44: 2845–2847. https://doi.org/10.1128/AAC.44.10.2845-2847.2000
19. Desbois AP, Coote PJ (2011) Bactericidal synergy of lysostaphin in combination with antimicrobial peptides. *Eur J Clin Microbiol Infect Dis* 30: 1015–1021. https://doi.org/10.1007/s10096-011-1188-z
20. Sadeghi S, Bakhshandeh H, Ahangari Cohan R, et al. (2019) Synergistic anti-staphylococcal activity of niosomal recombinant lysostaphin-LL-37. *Int J Nanomedicine* 14: 9777–9792. https://doi.org/10.2147/IJN.S230269
21. Korobov VP, Lemkina LM, Polyudova TV, et al. (2010) Isolation and characterization of a new low-molecular antibacterial peptide of the lantibiotics family. *Microbiology* 79: 206–215. https://doi.org/10.1134/S0026261710020128
22. Yaburova EV, Nechaeva YuI, Kononova LI, et al. (2026) Genome analysis of bacteria *Staphylococcus cohnii* VKM B-3165 with high susceptibility to antimicrobial compounds. *Microbiology* 95: 44–53. https://doi.org/10.1134/S0026261725602830
23. Korobov VP, Lemkina LM, Polyudova TV (2022) The mechanism of antibacterial action of the lantibiotic warnerin. *Microbiology* 91: 184–191. https://doi.org/10.1134/S0026261722020059
24. Bankevich A, Nurk S, Antipov D, et al. (2012) SPAdes: A new genome assembly algorithm and its applications to single-cell sequencing. *J Comput Biol* 19: 455–477. https://doi.org/10.1089/cmb.2012.0021
25. Gurevich A, Saveliev V, Vyahhi N, et al. (2013) QUAST: Quality assessment tool for genome assemblies. *Bioinformatics* 29: 1072–1075. https://doi.org/10.1093/bioinformatics/btt086
26. Parks DH, Imelfort M, Skennerton CT, et al. (2015) CheckM: Assessing the quality of microbial genomes recovered from isolates, single cells, and metagenomes. *Genome Res* 25: 1043–1055. https://doi.org/10.1101/gr.186072.114
27. Seemann T (2014) Prokka: Rapid prokaryotic genome annotation. *Bioinformatics* 30: 2068–2069. https://doi.org/10.1093/bioinformatics/btu153

28. Schwengers O, Jelonek L, Dieckmann MA, et al. (2021) Bakta: Rapid and standardized annotation of bacterial genomes via alignment-free sequence identification. *Microb Genom* 7. https://doi.org/10.1099/mgen.0.000685
29. Blin K, Shaw S, Vader L, et al. (2025) antiSMASH 8.0: Extended gene cluster detection capabilities and analyses of chemistry, enzymology, and regulation. *Nucleic Acids Res* 53: W32–W38. https://doi.org/10.1093/nar/gkaf334
30. van Heel AJ, de Jong A, Song C, et al. (2018) BAGEL4: A user-friendly web server to thoroughly mine RiPPs and bacteriocins. *Nucleic Acids Res* 46: W278–W281. https://doi.org/10.1093/nar/gky383
31. Zdouc MM, Blin K, Louwen NLL, et al. (2025) MIBiG 4.0: Advancing biosynthetic gene cluster curation through global collaboration. *Nucleic Acids Res* 53: D678–D690. https://doi.org/10.1093/nar/gkae1115
32. CLSI (2015) Methods for Dilution Antimicrobial Susceptibility Tests for Bacteria That Grow Aerobically; Approved Standard—Tenth Edition. CLSI document M07-A10. Wayne, PA: Clinical and Laboratory Standards Institute.
33. Lobanov A, Eroshenko D, Esaev A, et al. (2026) Antibacterial activity of lantibiotics, alone and in combination with colistin, against Gram-negative bacteria. *Arch Microbiol* 208: 275. https://doi.org/10.1007/s00203-026-04820-x
34. Kamp M, Hooven HW, Konings RNH, et al. (1995) Elucidation of the primary structure of the lantibiotic epilancin K7 from *Staphylococcus epidermidis* K7: Cloning and characterisation of the epilancin-K7-encoding gene and NMR analysis of mature epilancin K7. *Eur J Biochem* 230: 587–600. https://doi.org/10.1111/j.1432-1033.1995.tb20600.x
35. Velásquez JE, Zhang X, van der Donk WA (2011) Biosynthesis of the antimicrobial peptide epilancin 15X and its N-terminal lactate. *Chem Biol* 18: 857–867. https://doi.org/10.1016/j.chembiol.2011.05.007
36. Kusuma C, Jadanova A, Chanturiya T, et al. (2007) Lysostaphin-resistant variants of *Staphylococcus aureus* demonstrate reduced fitness *in vitro* and *in vivo*. *Antimicrob Agents Chemother* 51: 475–482. https://doi.org/10.1128/AAC.00786-06
37. Rohrer S, Ehlert K, Tschierske M, et al. (1999) The essential *Staphylococcus aureus* gene *fmhB* is involved in the first step of peptidoglycan pentaglycine interpeptide formation. *Proc Natl Acad Sci USA* 96: 9351–9356. https://doi.org/10.1073/pnas.96.16.9351
38. Łuszczki JJ, Wlaź A (2023) Isobolographic analysis of interactions—a pre-clinical perspective. *J Pre Clin Clin Res* 17: 238–241. https://doi.org/10.26444/jpccr/177246
39. Weidenmaier C, Peschel A, Kempf VAJ, et al. (2005) DltABCD- and MprF-mediated cell envelope modifications of *Staphylococcus aureus* confer resistance to platelet microbicidal proteins and contribute to virulence in a rabbit endocarditis model. *Infect Immun* 73: 8033–8038. https://doi.org/10.1128/IAI.73.12.8033-8038.2005
40. Vásquez A, Leidy C, Manrique-Moreno M (2025) Lysyl-phosphatidylglycerol: A lipid involved in the resistance of *Staphylococcus aureus* to antimicrobial peptide activity. *Antibiotics* 14: 349. https://doi.org/10.3390/antibiotics14040349



AIMS Press

© 2026 the Author(s), licensee AIMS Press. This is an open access article distributed under the terms of the Creative Commons Attribution License (https://creativecommons.org/licenses/by/4.0)